Supporting Information

Ittner *et al.* 10.1073/pnas.0808084105

SI Text

Histology and Immunohistochemistry. Immunohistochemistry on 3-μm sections of paraformaldehyde-fixed and paraffin-embedded tissue (1) was done using primary antibodies to tau (pS422 [Biosource], HT7, AT8, AT180, AT270 [all from Pierce]), ubiquitin (DAKO), porin (Molecular Probes), and TH (Sigma) and the ABC Elite Kit (Vector) or Alexa-labeled secondary antibodies (Molecular Probes) for visualization. Thiazin red staining together with AT8 immunofluorescence were performed as described (2). Neuromuscular junctions (NMJs) were stained with Alexa555-labeled α-bungarotoxin (Molecular Probes), together with porin or synaptophysin (Syp; Chemicon), on cryosections of calf muscles. Standard protocols were used for Gallyas, and Bielschowsky silver impregnations, and Thiazin red, Nissl, and hematoxylin and eosin staining.

Cell Counting and Quantification of Immunofluorescence Stainings. Stereologic analysis of TH-positive SN neurons was performed on serial sections as described (3). Immunofluorescence intensity was measured on images of randomly chosen areas taken with an IX81-X microscope (Olympus). Images were background-subtracted and analyzed for fluorescence intensity using MetaMorph 6.1 software (Molecular Devices). Sections were stained using Sequenza staining racks (Thermo) to standardize the procedure. For synaptic bouton counting, images were thresholded and numbers of synaptic boutons with an intensity greater than the threshold evaluated. Next, TH staining intensity in the SNc was measured for 25 randomly chosen neuronal cell bodies on four sections per genotype. Spinal cord α-motor neurons were counted on Nissl-stained cross sections.

Western Blotting. Proteins were extracted from brain areas using RIPA buffer (50 mM Tris pH 8.0, 150 mM sodium chloride, 1% Nonidet P-40, 5 mM EDTA, 0.5% sodium deoxycholate, and 0.1% SDS; all from Sigma) containing Complete protease inhibitor (Roche). Protein concentration was determined with the D_c-Protein Assay (Bio-Rad) to ensure equal gel loading. Sarkosyl-insoluble proteins were extracted from forebrains as previously described (4). For Western blotting (5), we used primary antibodies for tau (tau-5), APP, kinesin light chain, kinesin heavy chain, Syp, GAPDH, actin (all from Chemicon), tau phosphorylated at S422 (pS422; Biosource), human tau (HT7), tau phosphorylated at S202/T205 (AT8), at T231/S235 (AT180), at T181 (AT270) (Pierce), at S262/S356 (12E8; from Peter Seubert, Elan Pharmaceuticals, South San Francisco, CA), at S396/404 (PHF-1; from Peter Davies, Albert Einstein College of Medicine, New York, NY), growth-associated protein 43 (Gap43), synaptotagmin, kinesin family member 1A (all from Santa Cruz), Jip1 (Zymed), respiratory chain complexes I and V (Molecular Probes), amyloid β precursor-like proteins 1 and 2 (Calbiochem), presenilin 1 (Cell Signaling), and calcitonin gene-related peptide (Walter Born, University of Zurich, Zurich, Switzerland). Western blots were detected and quantified in a VersaDoc 4000 detection system (Bio-Rad).

Electron Microscopy. Anesthetized mice were perfused with 20 ml of cold PBS solution followed by 20 ml of 0.1 M phosphate buffer, pH 7.2, containing 4% paraformaldehyde and 3% glutaraldehyde. Sciatic nerves were postfixed overnight at 4°C. The nerves were then treated with 2% osmium tetroxide (Sigma), dehydrated by acetone (Sigma), and embedded in Spurr (Proscietech). For semithin sectioning, Spurr-embedded sciatic nerves were sectioned at 0.5 μm and stained with 0.1% toluidine blue (Sigma) according to standard procedures. For electron microscopy, nerves were sectioned at 60 nm, contrasted with uranyl acetate and lead citrate, and digital pictures were taken with a Philips CM12 electron microscope.

Sciatic Nerve Ligation. Sciatic nerve ligation was carried out as described (6, 7). Briefly, exposed right sciatic nerves of ketamine/xylazine-anesthetized mice were ligated with a thin surgical thread (Brand) and the wound subsequently closed with three suture clips (Fine Science Tools). Left sciatic nerves served as control. Six hours after surgery, mice were perfused with 4% paraformaldehyde for histology or nerves were harvested and proximal and distal parts were pooled from four mice for Western blot analysis.

Behavioral Testing. Memory function of 12 mice per group and age was tested in the novel object recognition task as described (8, 9). Briefly, after 3 days of habituation to the 40 $\times$ 30-cm arena, mice were exposed for 15 min to two different objects that were placed in opposite corners. The following day, one of the objects was replaced, and the mice were again exposed for 15 min.

Clasping of limbs was shown by lifting mice by their tails. Footstep length was measured by letting 8 K3 and 5 WT mice walk over a strip of white paper in a 5-cm-wide, 50-cm-long square tube, after coloring their front paws with red ink and their hind paws with blue ink. Tremor intensity was scored by two independent investigators, with 0 indicating no tremor, 1 indicating intermittent slight tremor, 2 indicating intermittent tremor, 3 indicating strong tremor with rare quiescent periods, and 4 indicating continuous tremor. The open field testing of 12 mice per group and age was done with automated tracking in a 40 $\times$ 30-cm arena over a period of 10 min. Rearing activity during open field testing was analyzed by manual counting from recordings by two independent and blinded persons. For the challenging beam test (10), 16 K3 and 8 WT mice had to cross a 4-mm-wide, 100-cm-long horizontal pole to reach the home cage. Slipping of the hind limbs was counted. K3 mice were then treated with a single i.p. injection of 100 mg/kg L-Dopa and tested again 30 min later. The cataleptic response to i.p. injections of haloperidol was analyzed in the bar test (11). Thirty minutes after injection, the front paws were placed on a 3-mm-thick horizontal bar that was mounted 4 cm above bench-top level. The time both paws remained on the bar together with arrested whisker movement was recorded with a time out of 180 seconds. The response to increasing concentrations was tested with 2-day injection-free intervals to avoid haloperidol accumulation. Tests were recorded with an MV690 digital camera (Canon). All tests were preceded by 2 days of training sessions.

Dopamine Measurement. Brains were analyzed by HPLC as reported previously (12).

Stereotaxic Injections. Stereotaxic injection of 0.5 μl of a 5% Fluoro-Gold (Fluorochrome) solution in 0.9% saline solution (Sigma) into the right caudate putamen (i.e., striatum) of ketamine/xylazine-anesthetized mice (7 K3 and 7 WT mice) was carried out in a Model 900 stereotaxic frame (David Kopf Instruments). The injection site relative to the bregma was calculated according to the Paxinos Mouse Brain Atlas (13) with coordinates as follows: x, -1.75 mm; y, -3.5 mm; z, 1.0 mm. The injection was done for 5 min, with the needle remaining for a

further 5 min before it was slowly removed, and the skin was closed with three suture clips. Four days after surgery, anesthetized mice were perfused as described earlier. Brains were embedded in paraffin and sectioned as described earlier. Series of 10-μm sections were analyzed for accumulation of Fluoro-Gold in SNc cell bodies immediately after sectioning. The injection site was confirmed by hematoxylin and eosin staining.

1. Ittner LM, *et al.* (2005) Compound developmental eye disorders following inactivation of TGFbeta signaling in neural-crest stem cells. *J Biol* 4:11.
2. Uchihara T, *et al.* (2001) Different conformation of neuronal tau deposits distinguished by double immunofluorescence with AT8 and thiazin red combined with Gallyas method. *Acta Neuropathol* 102:462–466.
3. Gotz J, Chen F, van Dorpe J, Nitsch RM (2001) Formation of neurofibrillary tangles in P301l tau transgenic mice induced by Abeta 42 fibrils. *Science* 293:1491–1495.
4. Goedert M, Spillantini MG, Cairns NJ, Crowther RA (1992) Tau proteins of Alzheimer paired helical filaments: Abnormal phosphorylation of all six brain isoforms. *Neuron* 8:159–168.
5. Ittner LM, Koller D, Muff R, Fischer JA, Born W (2005) The N-terminal extracellular domain 23–60 of the calcitonin receptor-like receptor in chimeras with the parathyroid hormone receptor mediates association with receptor activity-modifying protein 1. *Biochemistry* 44:5749–5754.
6. Hirokawa N, Sato-Yoshitake R, Yoshida T, Kawashima T (1990) Brain dynein (MAP1C) localizes on both anterogradely and retrogradely transported membranous organelles in vivo. *J Cell Biol* 111:1027–1037.
7. Kamal A, Almenar-Queralt A, LeBlanc JF, Roberts EA, Goldstein LS (2001) Kinesin-mediated axonal transport of a membrane compartment containing beta-secretase and presenilin-1 requires APP. *Nature* 414:643–648.
8. Ennaceur A, Delacour J (1988) A new one-trial test for neurobiological studies of memory in rats. 1: Behavioral data. *Behav Brain Res* 31:47–59.
9. Bevins RA, Besheer J (2006) Object recognition in rats and mice: A one-trial non-matching-to-sample learning task to study 'recognition memory'. *Nat Protocols* 1:1306–1311.
10. Goldberg MS, *et al.* (2003) Parkin-deficient mice exhibit nigrostriatal deficits but not loss of dopaminergic neurons. *J Biol Chem* 278:43628–43635.
11. Sotnikova TD, *et al.* (2005) Dopamine-independent locomotor actions of amphetamines in a novel acute mouse model of Parkinson disease. *PLoS Biol* 3:e271.
12. Gurtman CG, Morley KC, Li KM, Hunt GE, McGregor IS (2002) Increased anxiety in rats after 3,4-methylenedioxymethamphetamine: association with serotonin depletion. *Eur J Pharmacol* 446:89–96.
13. Paxinos G, Franklin KBJ (2001) *The Mouse Brain in Stereotaxic Coordinates* (Academic, San Diego).

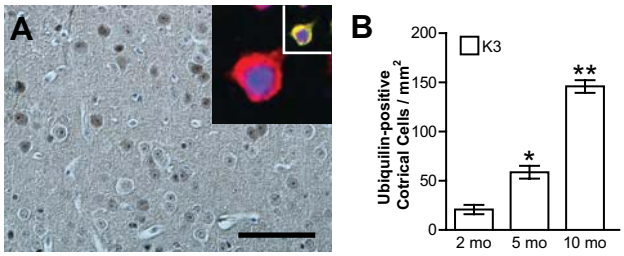

Fig. S1. Ubiquinated tau in K3 cortical neurons. (*A*) Cortical neurons of K3 mice stain for ubiquitin at 10 months of age. *Large inset*, ubiquitin staining (red) co-localizes with AT180 phosphorylated tau (green, not shown), as shown by merging (yellow, *small inset*). Scale bar, 100 μm. (*B*) Numbers of ubiquitin-positive cells progressively increase with age in K3 mice (*, $P < 0.01$ and **, $P < 0.0001$ vs. previous values).

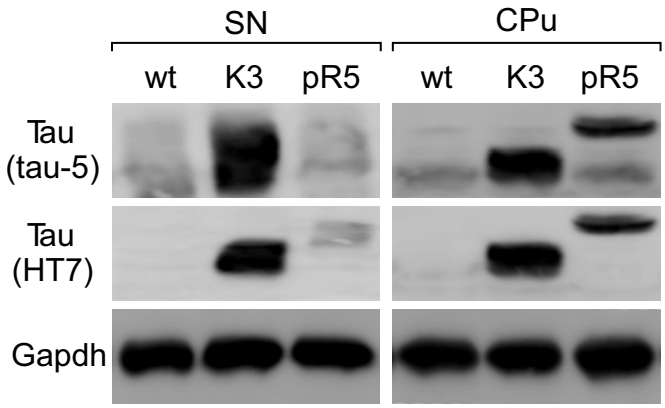

Fig. S2. K369I tau is expressed in the SN of K3 mice. Comparison of brain regions in WT, K3, and P301L tau transgenic pR5 mice that lack Parkinsonism by Western blotting reveals that only K3 mice express transgenic tau in the SN. Transgene expression in other brain regions including the striatum (CPu) is comparable in K3 and pR5 mice.

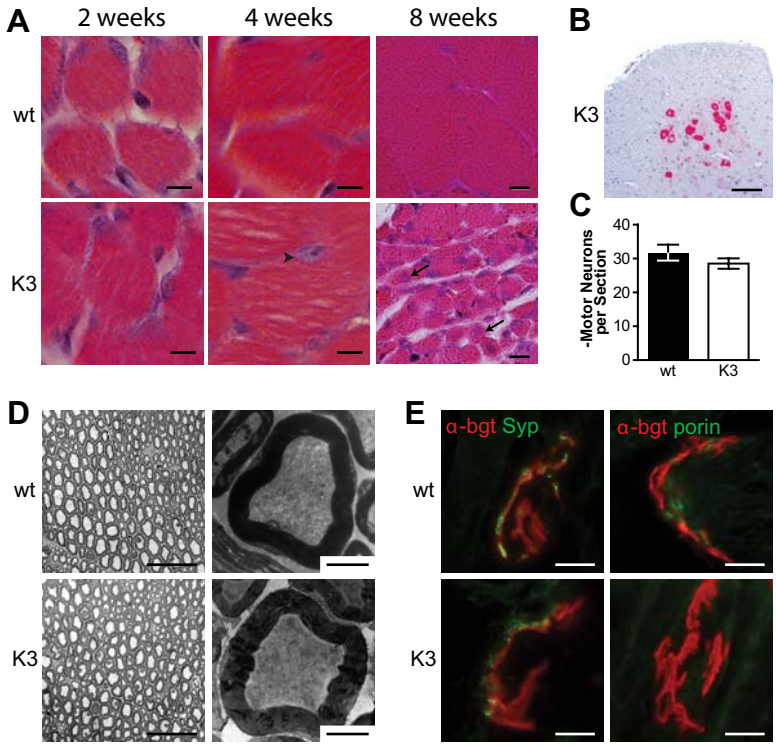

Fig. S3. Amyotrophy in K3 mice occurs in the absence of overt neurodegeneration. (*A*) In 2-week-old K3 and WT littermates, muscles, including calf muscle, are morphologically indistinguishable. Muscles from 4-week-old K3 mice present with swollen nuclei (arrowhead) as first signs of degeneration. At 8 weeks of age, K3 muscles show degenerating cell bundles and multiple swollen and centralized nuclei (arrows), both of which are signs of neurogenic muscle degeneration. (Scale bars, 25 μm.) (*B*) Immunohistochemistry of spinal cord cross sections shows that anterior horn α-motor neurons express transgenic tau (red). (Scale bar, 100 μm.) (*C*) Numbers of anterior horn α-motor neurons in spinal cords are not reduced even in 1-year-old K3 mice compared with WT mice ($P = 0.231$). (*D*) Absence of overt neuronal cell loss revealed by lack of signs of degeneration as assessed by light microscopy (*Left*) and electron microscopy (*Right*) of sciatic nerves of 1-year-old K3 mice. (Scale bars, 40 μm (*Left*) and 2 μm (*Right*).) (*E*) Normal appearance of neuromuscular junctions (NMJs) shown by co-staining for presynaptic synaptophysin (Syp, green) and postsynaptic α-bungarotoxin (α-bgt; red, *Left*). However, co-staining with α-bgt (red) and the mitochondrial protein porin (green) shows less mitochondria in K3 NMJs compared with WT controls, suggesting that K3 NMJs are functionally impaired. (Scale bar, 10 μm.)

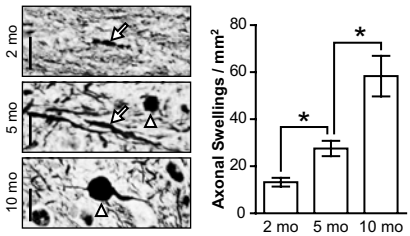

Fig. S4. Axonal swellings and spheroids in K3 mice. Axonal swellings (arrows) in 2-month-old K3 mice are an early morphological correlate of axonal transport defects in the nigrostriatal projection. Furthermore, with disease progression, axonal spheroids (arrowheads) are found in the nigrostriatal projection at 5 months, and are more pronounced in 10-month-old K3 mice (*, $P < 0.001$). No swellings and spheroids are found in WT littermates (not shown). (Scale bar, 10 μm.)

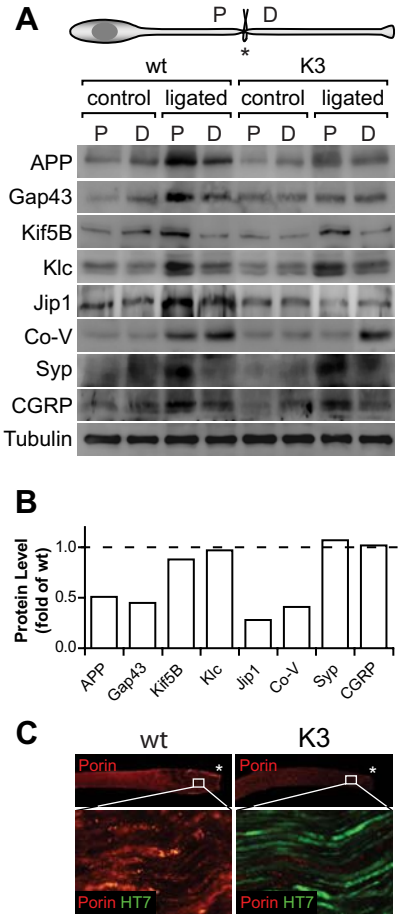

Fig. S5. K3 mice show impaired anterograde axonal transport in sciatic nerves. (*A*) Axonal transport assessed directly by unilateral ligation of sciatic nerves from WT and K3 mice. Proximal (P) and distal (D) parts of ligated and control nerves were analyzed for the accumulation of anterogradely and retrogradely transported proteins by Western blotting of pooled nerves. Decreased accumulation of proteins indicates reduced transport. Markers of different transport vesicles (APP, Gap43, Syp, and CGRP); mitochondrial protein (i.e., respiratory chain complex V); proteins of the kinesin-1 motor complex (kinesin heavy chain (Kif5B), kinesin light chain (KLC), and Jip1); and tubulin. (*B*) Quantification of levels proximal to the ligation of pools of K3 sciatic nerves presented as expression (in fold) compared with WT (dashed line). (*C*) Immunohistochemistry of proximal (P) parts of ligated sciatic nerves in K3 mice shows that those axons that express transgenic tau (i.e., HT7) do not accumulate mitochondria as determined with an antibody for porin. In contrast, axons without transgenic tau (arrow) accumulate mitochondria proximal to the ligation (asterisk), as in WT littermates.

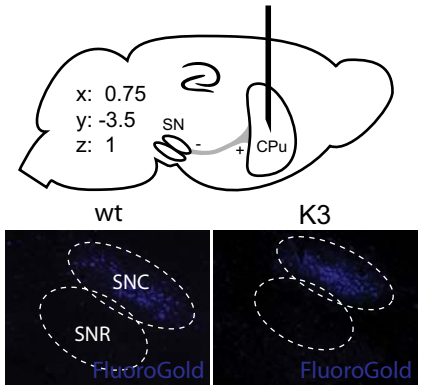

Fig. S6. Retrograde transport of FluoroGold is normal in K3 mice. FluoroGold dye was stereotaxically injected into the striatum (CPu) of 3-month-old mice at positions x (0.75 mm), y (−3.5 mm), and z (1 mm) according to the bregma. Retrograde transport of the dye was unaffected in K3 mice, as shown by equal dye recovery in neurons of the SNc in K3 mice and WT littermates.